The XXVII International Scientific Conference of Young Scientists and Specialists (AYSS-2023)

STRUCTURES AND PHASE TRANSITIONS IN TERNARY Fe-BASED ALLOYS
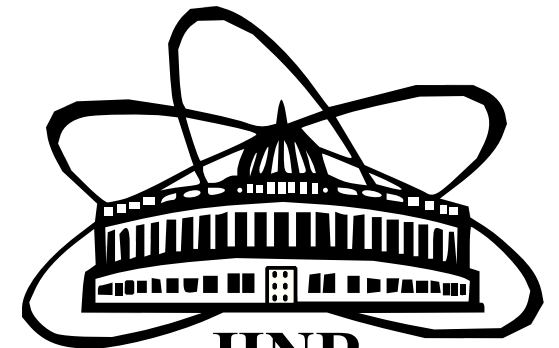
Yerzhanov Bekarys

Postgraduate student of KFU IP
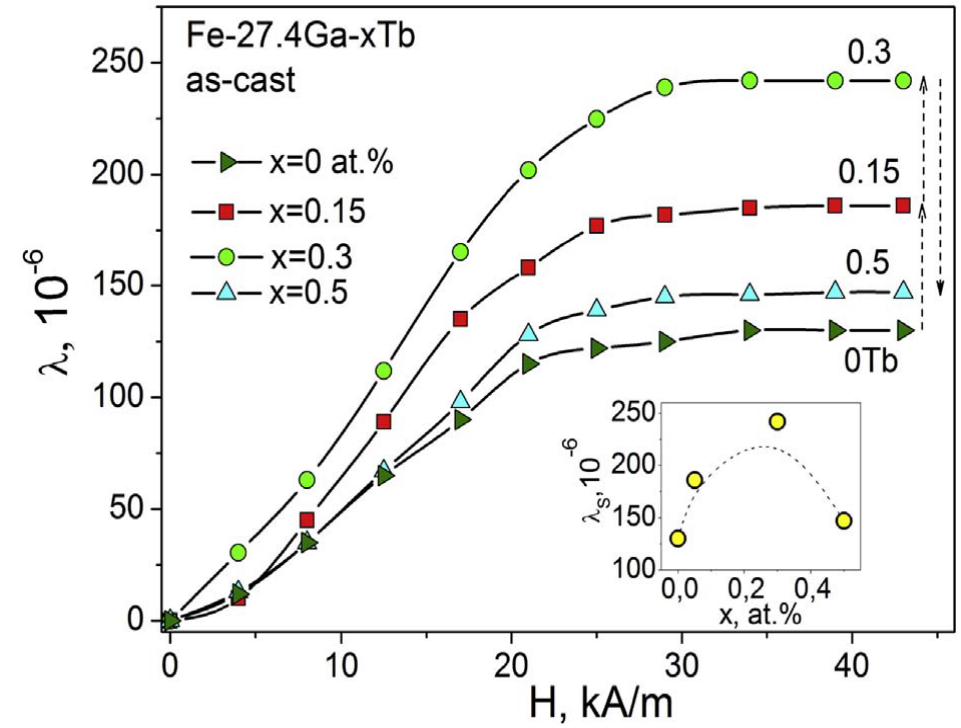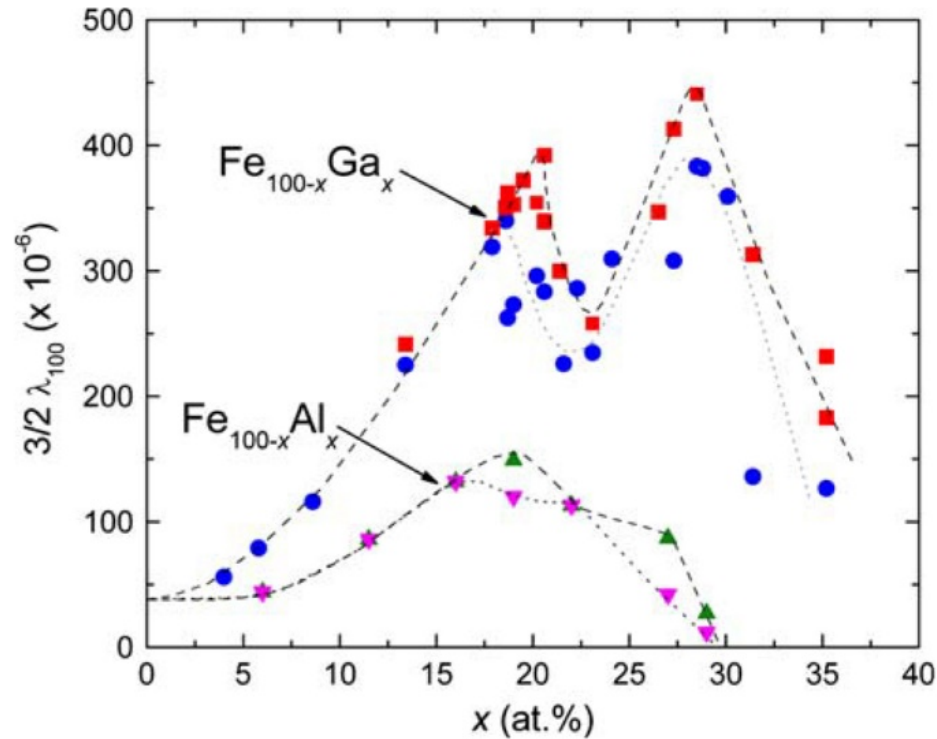
1.3.8 Condensed matter physics

Trainee researcher

(under the supervision of Dr. A.M. Balagurov)

FLNP JINR

JINR
FLNP
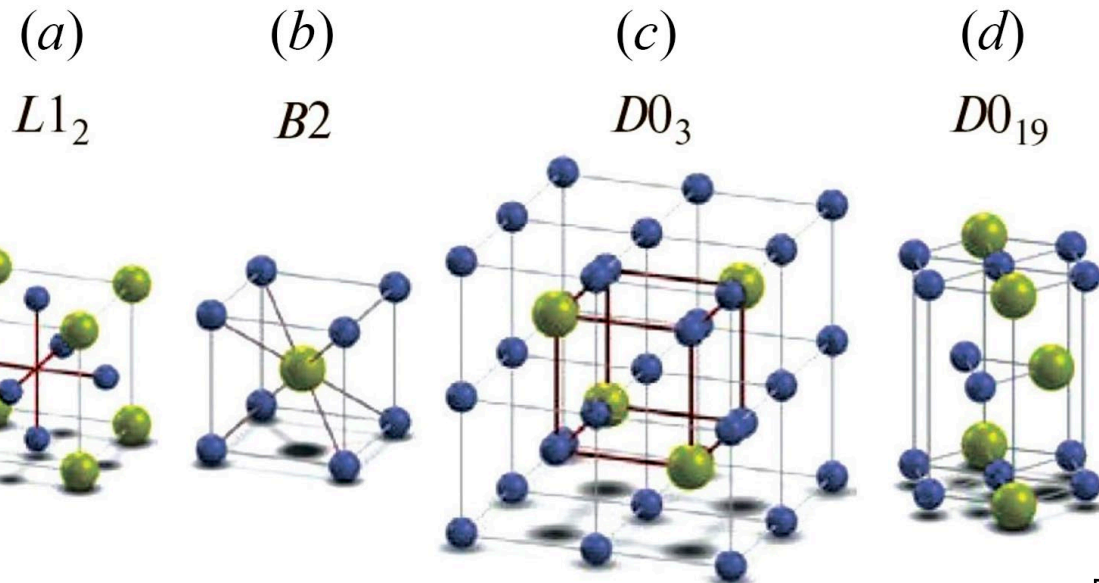
Magnetostrictive properties of Fe-based systems

Magnetostriction dependence for Fe–Ga and Fe–Al alloys. The blue circles and pink triangles show the values after the samples were cooled in an oven at a rate of 600°C/h. Red squares and green triangles indicate holding in an oven for 4 h followed by quenching in water from 1000°C [1].

Parallel magnetostriction vs. applied magnetic field, λ(H), curves for the as-cast Fe-27.4Ga-xTb (x = 0.15, 0.3, and 0.5 at.%) samples. Inset shows the dependence of the saturation magnetostriction, λ_S, on the Tb content at room temperature [2].

1. Magnetostriction of binary and ternary Fe-Ga alloys / E.M. Summers, T.A. Lograsso, M. Wun-Fogle // J. Mater. Sci.
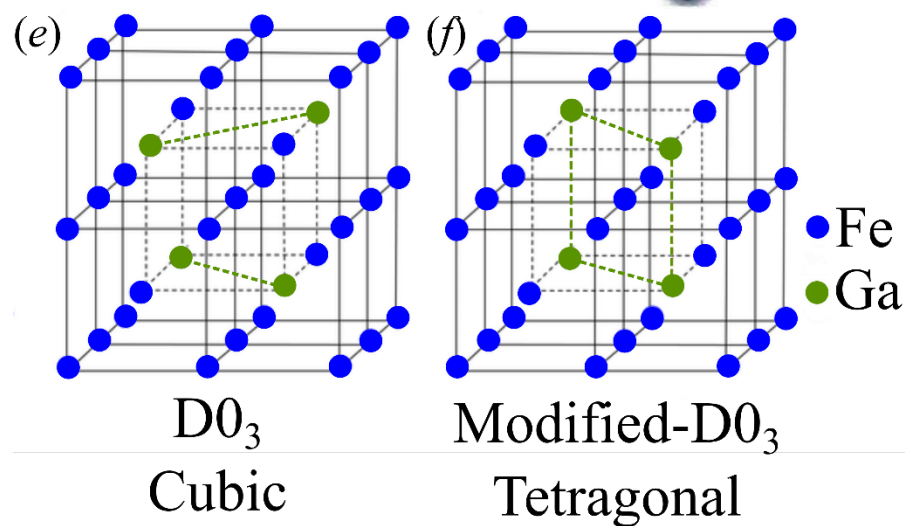
2. Tb-dependent phase transitions in Fe-Ga functional alloys / A. Emdadi [et al.] // Intermetallics

Structures discovered in Fe-Ga based systems

(*a*)

$L1_2$

(*b*)
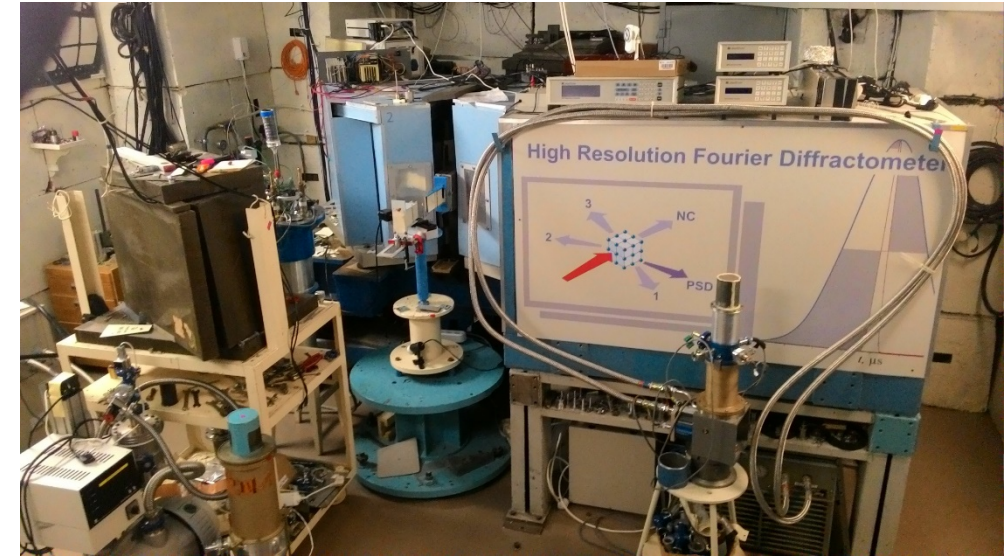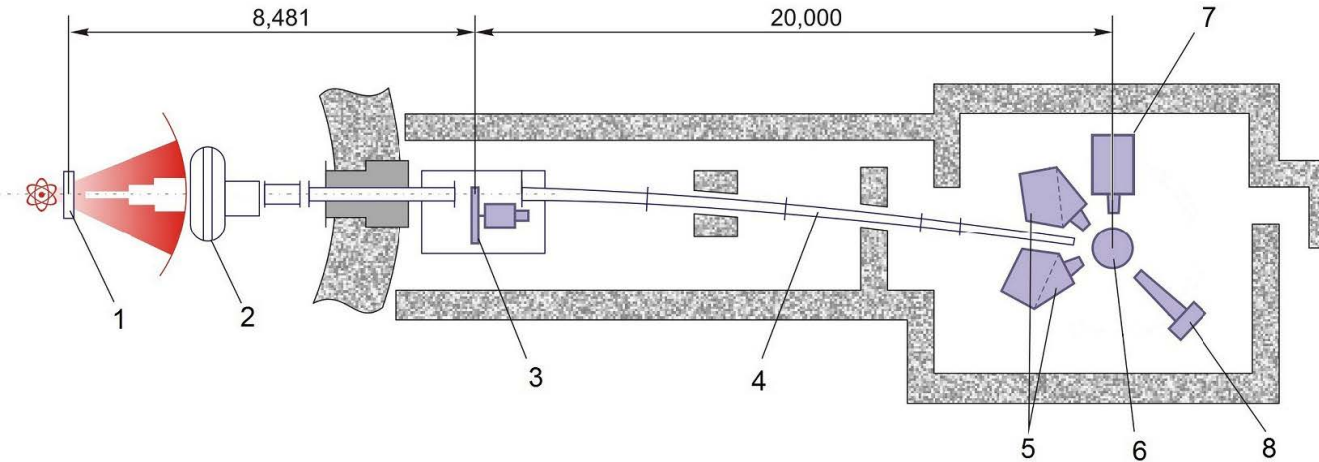
$B2$

(*c*)

$D0_3$

(*d*)

$D0_{19}$

Unit cells of phases in Fe–Ga systems:

$L1_2$ (a), B2 (b), $D0_3$ (c), $D0_{19}$ (d). Green balls are gallium or aluminum atoms, blue balls are iron atoms.

(*e*)

(*f*)

$D0_3$
Cubic

Modified-$D0_3$
Tetragonal

• Fe
• Ga

Lattice type	Symmetry	Space group	Basic lattice
A1	Cubic	Fm3m	HCC
A2	Cubic	Im3m	BCC
A3	Hexagonal	P6$_3$/mmc	HCP
B2	Cubic	Pm3m	BCC
D0$_3$	Cubic	Fm3m	BCC
Ll$_2$	Cubic	Pm3m	HCC
D0$_{19}$	Hexagonal	P6$_3$/mmc	HCP

$$a(D0_3) \approx 2a(B2)$$

High resolution neutron Fourier diffractometry

HRFD configuration at the IBR-2 reactor:

1 – water moderator;

2 – Background chopper;

3 – Fourier chopper;

4 – curved mirror neutron guide;

5 – backscatter detectors ($2\theta = \pm152°$);

6 – place of the sample;

7 – detector at $2\theta = 90°$;

8 – position-sensitive detector at $2\theta = 30°$.

Basic parameters

High resolution
- Neutron flux at sample position
- Resolution ($\Delta d/d$) for $2\theta = 152°$,
- Acquisition time

d_{hkl}: $0.6 - 4$ Å
$3\cdot10^6$ n/cm²/s
$\Delta d/d \approx 0.0015$
1 hour

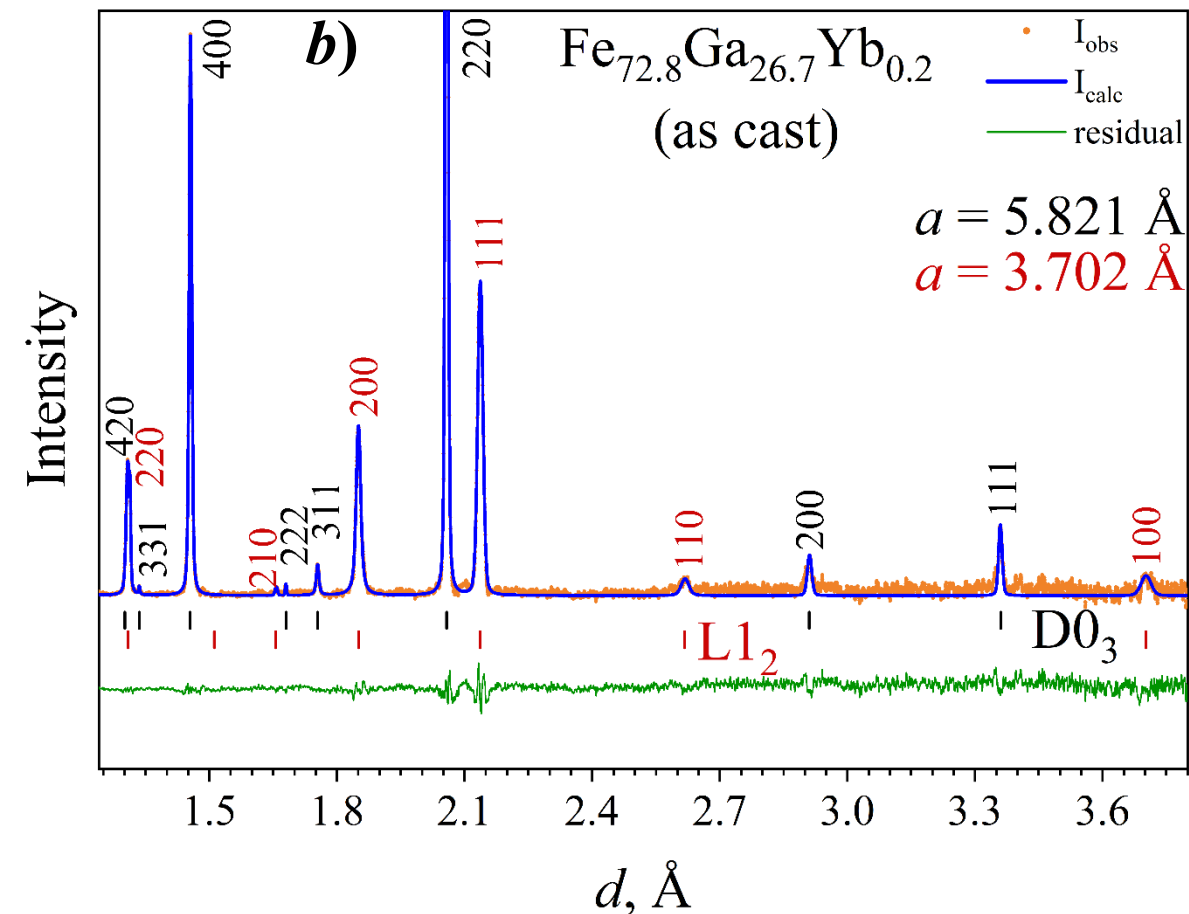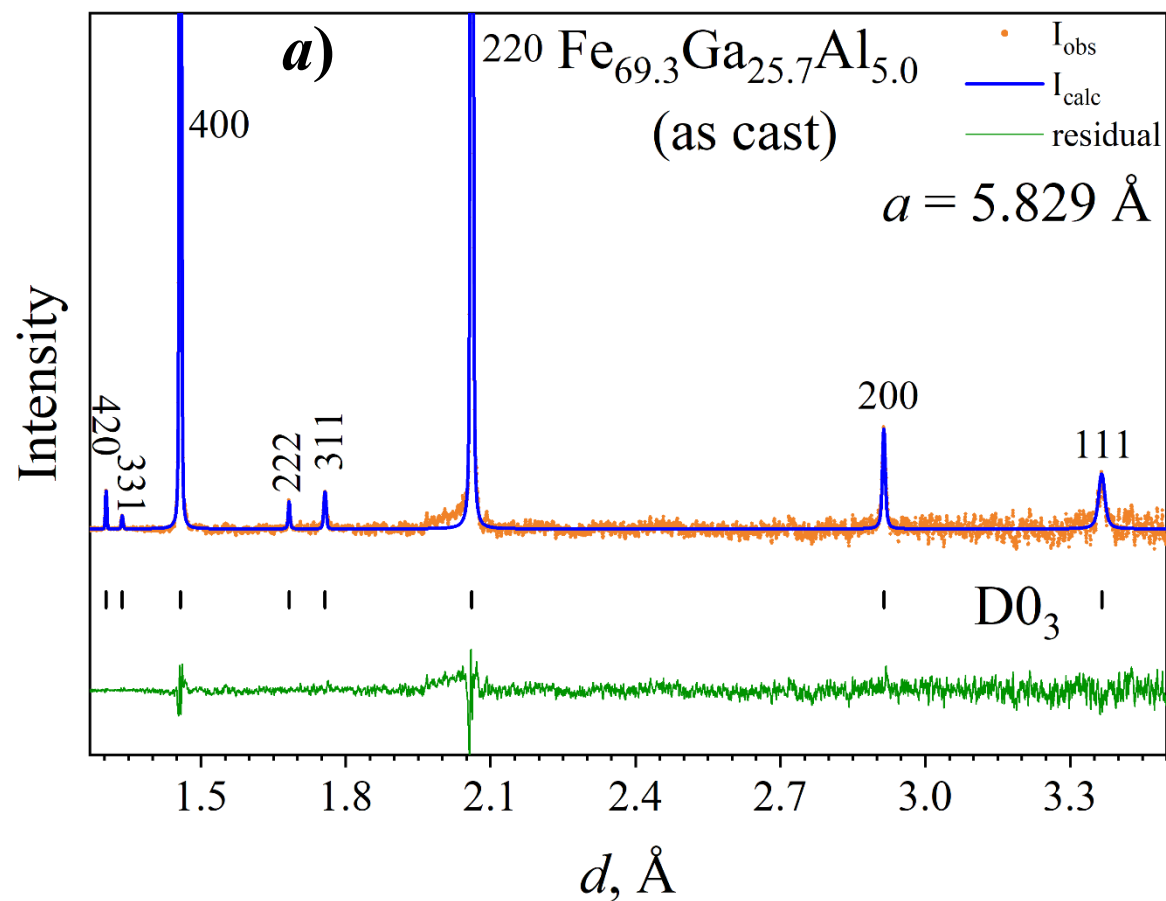**Medium Resolution (High intensity)**
- Neutron flux at sample position
- Resolution ($\Delta d/d$) for $2\theta = 152°$,
- Acquisition time
- <u>Standard sample volume</u>

d_{hkl}: $2 - 16$ Å
$1.4 \cdot 10^7$ n/cm²/s
$\Delta d/d \approx 0.015$
1 minute
~ 2 cm³

4. High-resolution neutron Fourier diffractometer at the IBR-2 pulsed reactor: A new concept / A. Balagurov [et al.] // Nuclear Inst. and Methods in Physics Research B
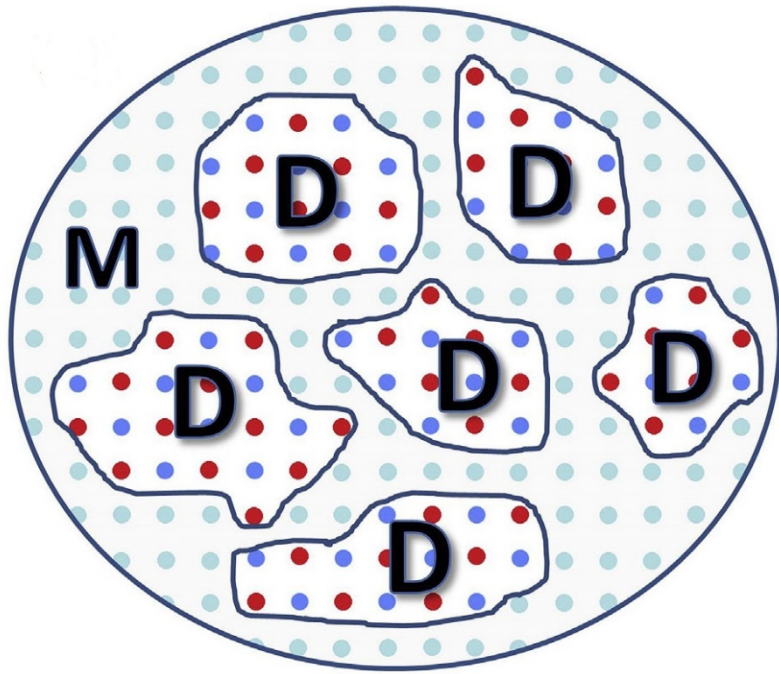
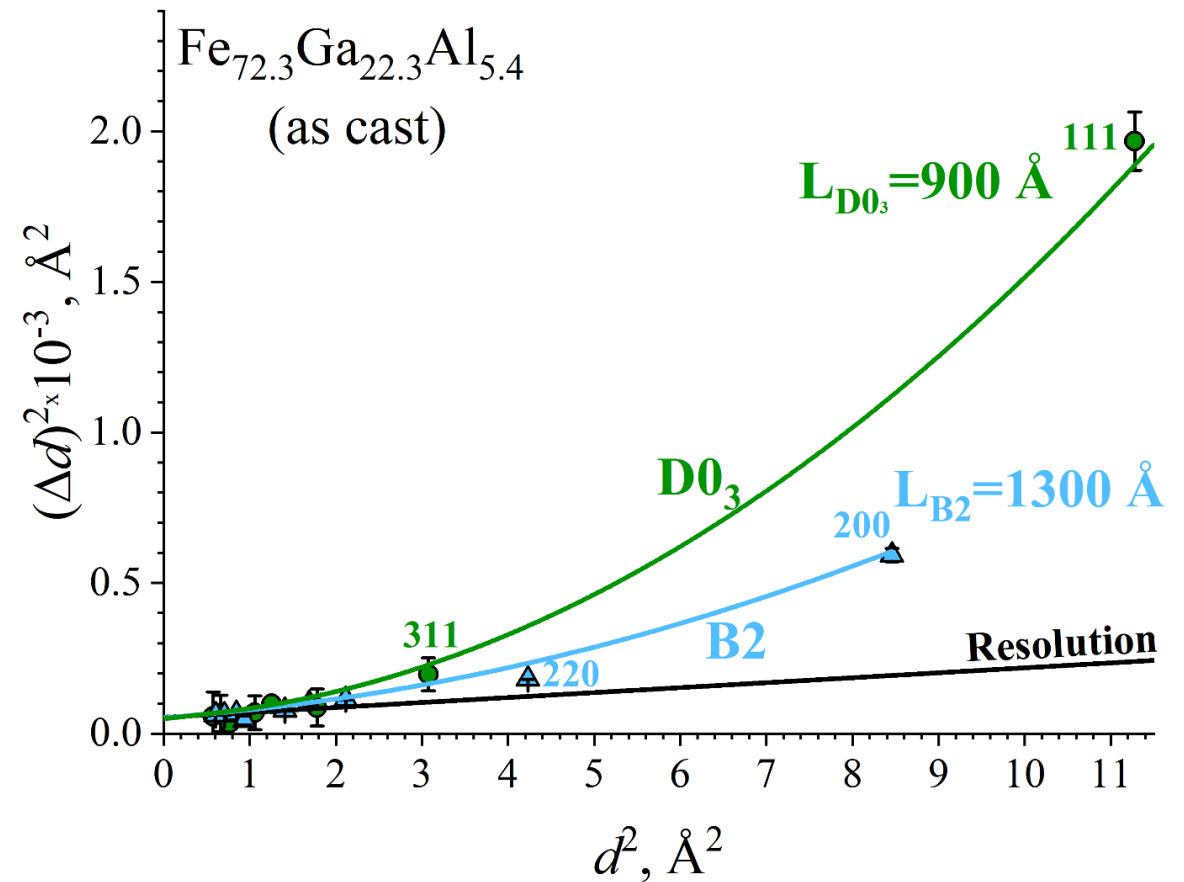# High resolution neutron diffraction patterns of Fe-Ga based alloys

In the neutron diffraction pattern of FeGaAl(***a***) alloy the $D0_3$ structure in the initial state was discovered. FeGaYb(***b***) alloy is distinguished by the presence of both $D0_3$ and $L1_2$ structures in the initial state.

Graphs of the Williamson-Hall analysis of Fe-Ga based alloys

$$\Delta d = \frac{d^2}{L} \cdot \frac{h+k+l}{\sqrt{(h^2+k^2+l^2)}}$$

The graph shows how the widths of the peaks belonging to the phases B2 and $D0_3$ lie on separate parabolas. The obtained values were analyzed by the Williamson-Hall method, which made it possible to qualitatively estimate the values of the coherent scattering domains (**CSD**) of two phases. The two-phase state is organized form of a matrix, B2, in which clusters of the $D0_3$

5. Antiphase domains or dispersed clusters? Neutron diffraction study of coherent atomic ordering in Fe_3Al-type alloys / A. M. Balagurov [et al.] // Acta Materialia.

Method (Pielaszek) for estimating the size distribution of coherently scattering domain size

It is assumed that the size of the crystallites is distributed in accordance with the gamma distribution, which allows one to obtain virtually the same information as using Fourier analysis of profiles of peaks.
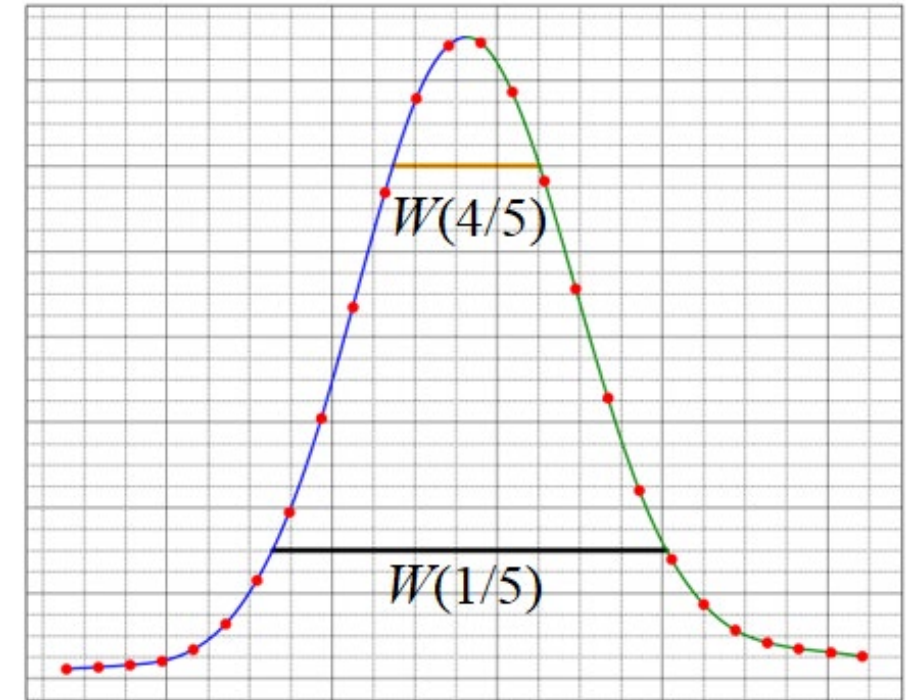
$<R> = 2BC/W(4/5)$, $\sigma = 2BC^{1/2}/W(4/5)$,

$A = \text{arcctg}(277069 - 105723 \times W(1/5)/W(4/5))$,

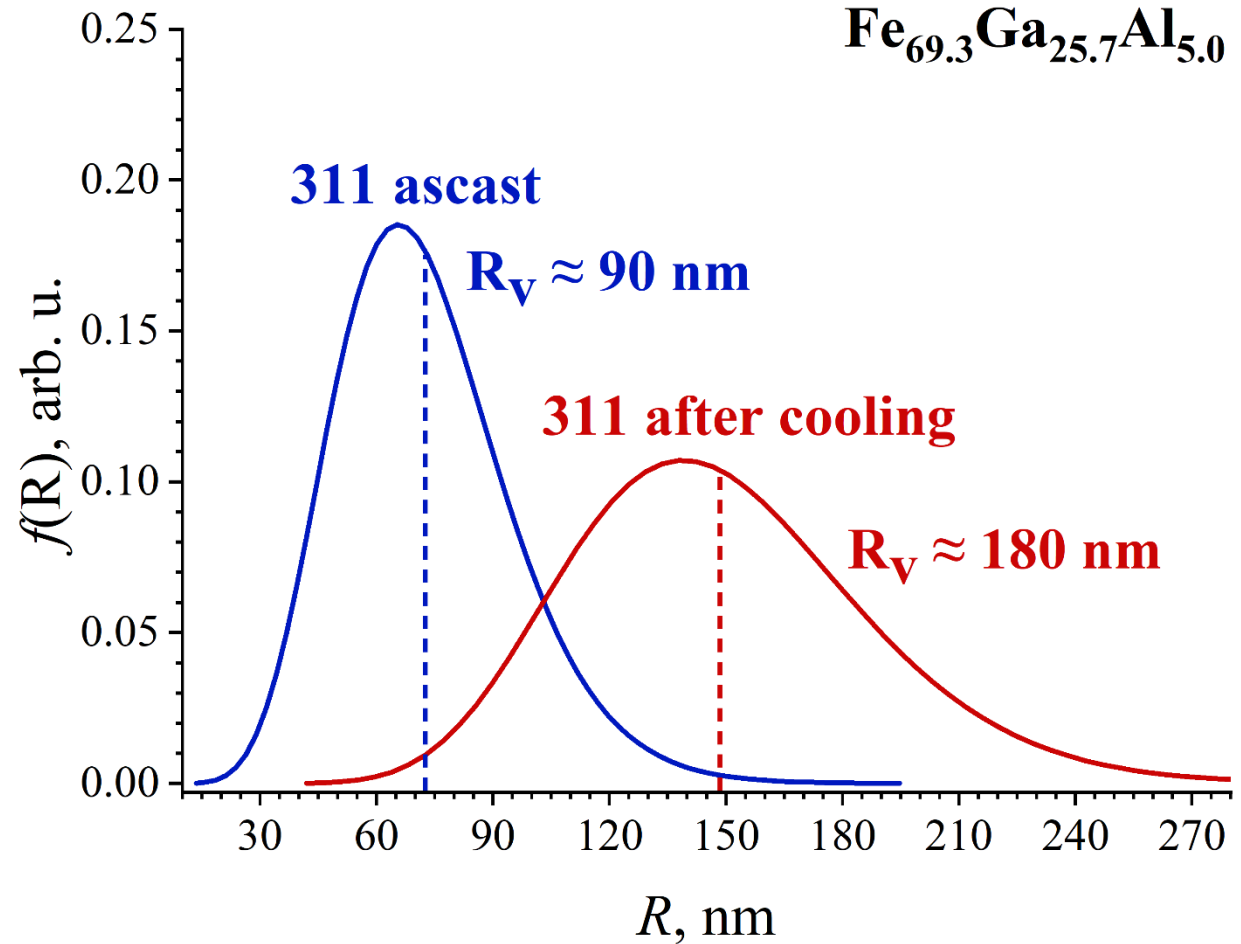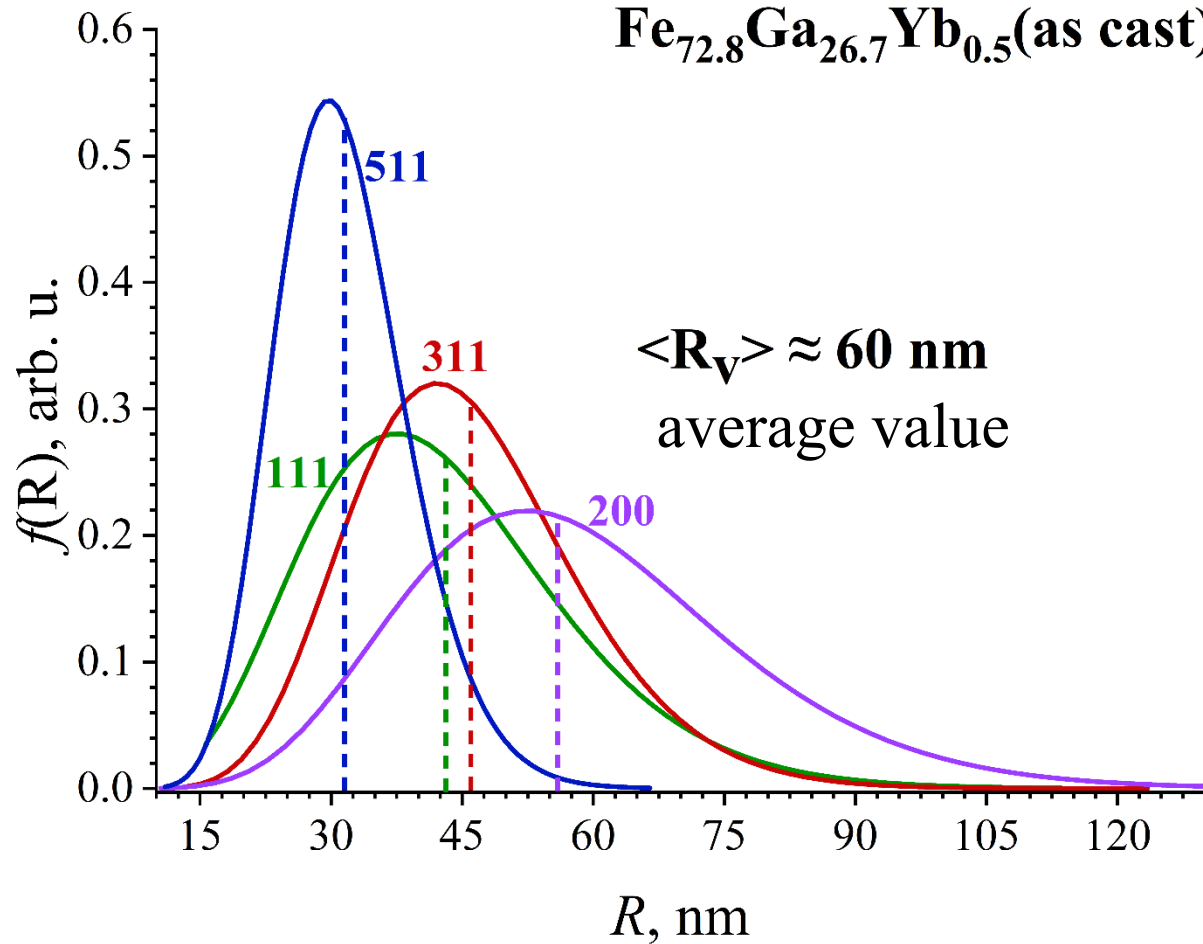$B = 0.001555 + 0.00884 \times \text{ctg}(0.002237 - 2101 \times A)$,

$C = -0.6515 - 463695 \times A$.

Method for determining peak widths at levels of 1/5 and 4/5 amplitude.

The author derived formulas that allow to calculate the coherently scattering domain size and dispersion by determining the full peak widths at levels 1/5 and 4/5 amplitude, W(1/5) and W(4/5)

6. $FW\frac{1}{5}/\frac{4}{5}M$ method for determination of the grain size distribution from powder diffraction line profile/ Roman Pielaszek. // J. Alloys Compd. (2004). 382, 128–132.
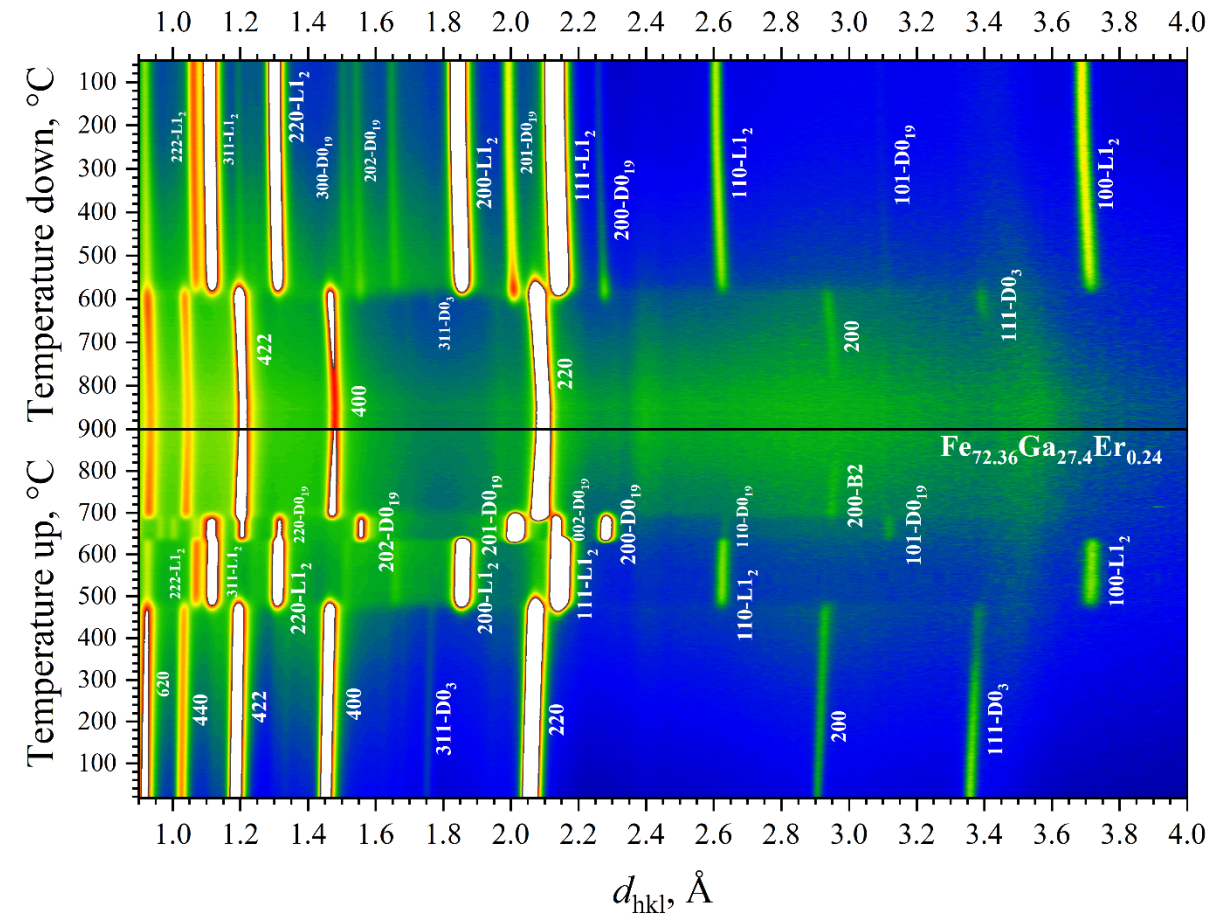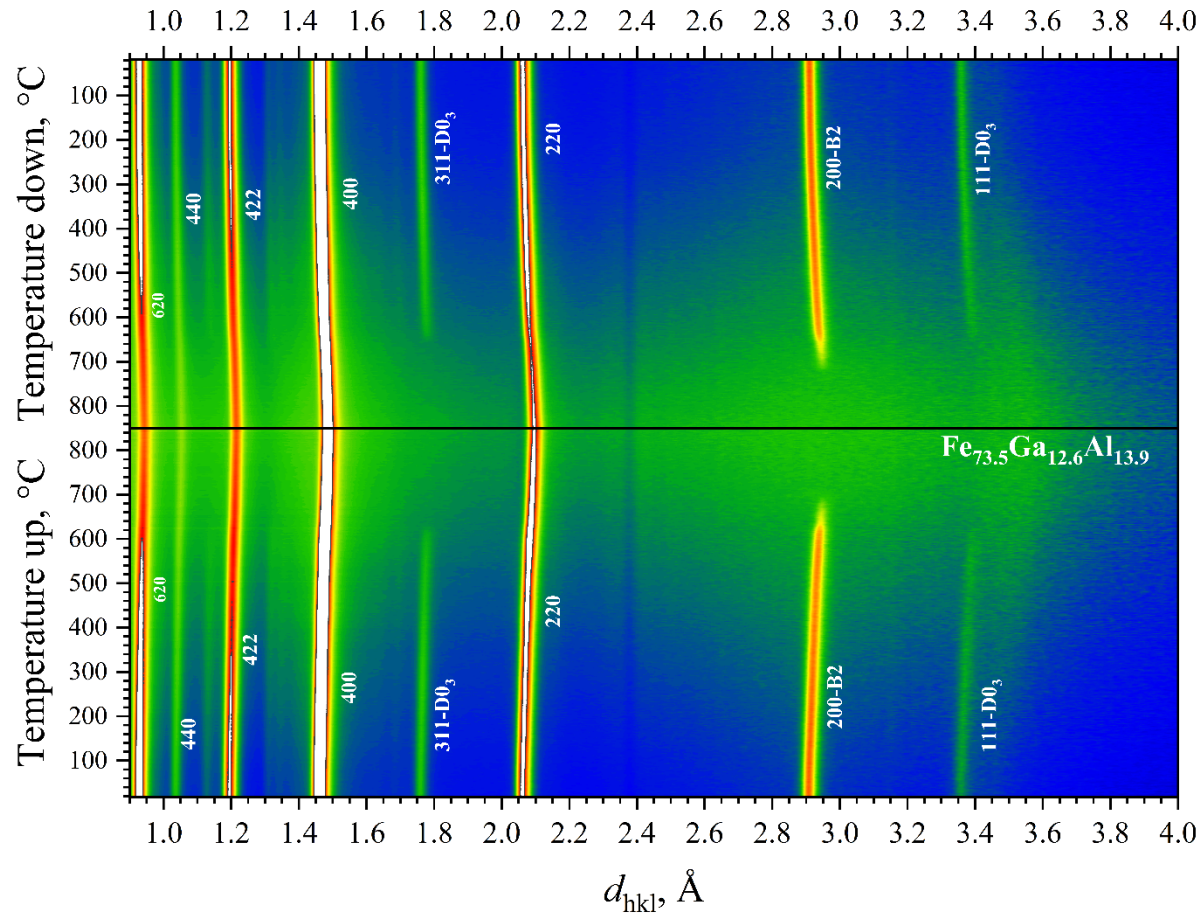
Method (Pielaszek) for estimating the size distribution of coherently scattering domain size

Here the result of applying this method on obtained neutron diffraction spectra of polycrystalline Fe-based samples is presented. Fe-Ga-Al alloy, after an experiment with slow heating and cooling, the CSD size of the clusters with $D0_3$ phase doubled.
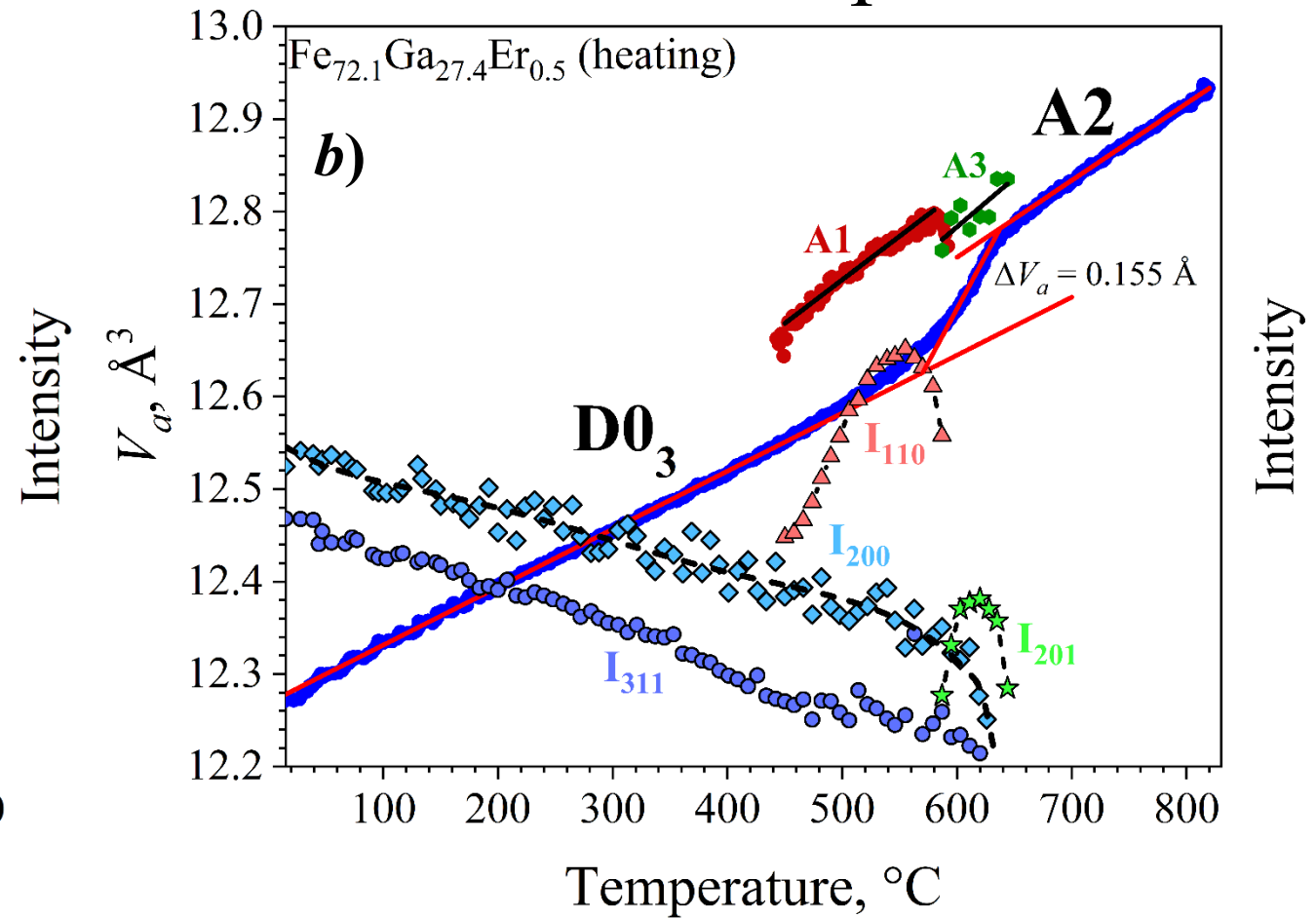
Analysis of the data of the thermodiffractometric experiment

$Fe_{73.5}Ga_{12.6}Al_{13.9}$

$Fe_{72.36}Ga_{27.4}Er_{0.24}$

Neutron diffraction spectra of alloys based on Fe-Ga, measured during its continuous heating and subsequent cooling at a rate of ±2 ºC/min. The temperature axis is directed from bottom to top. The 2D map contains around 900 individual diffraction spectra with a measurement time of 1 minute.

Analysis of the data of the thermodiffractometric experiment

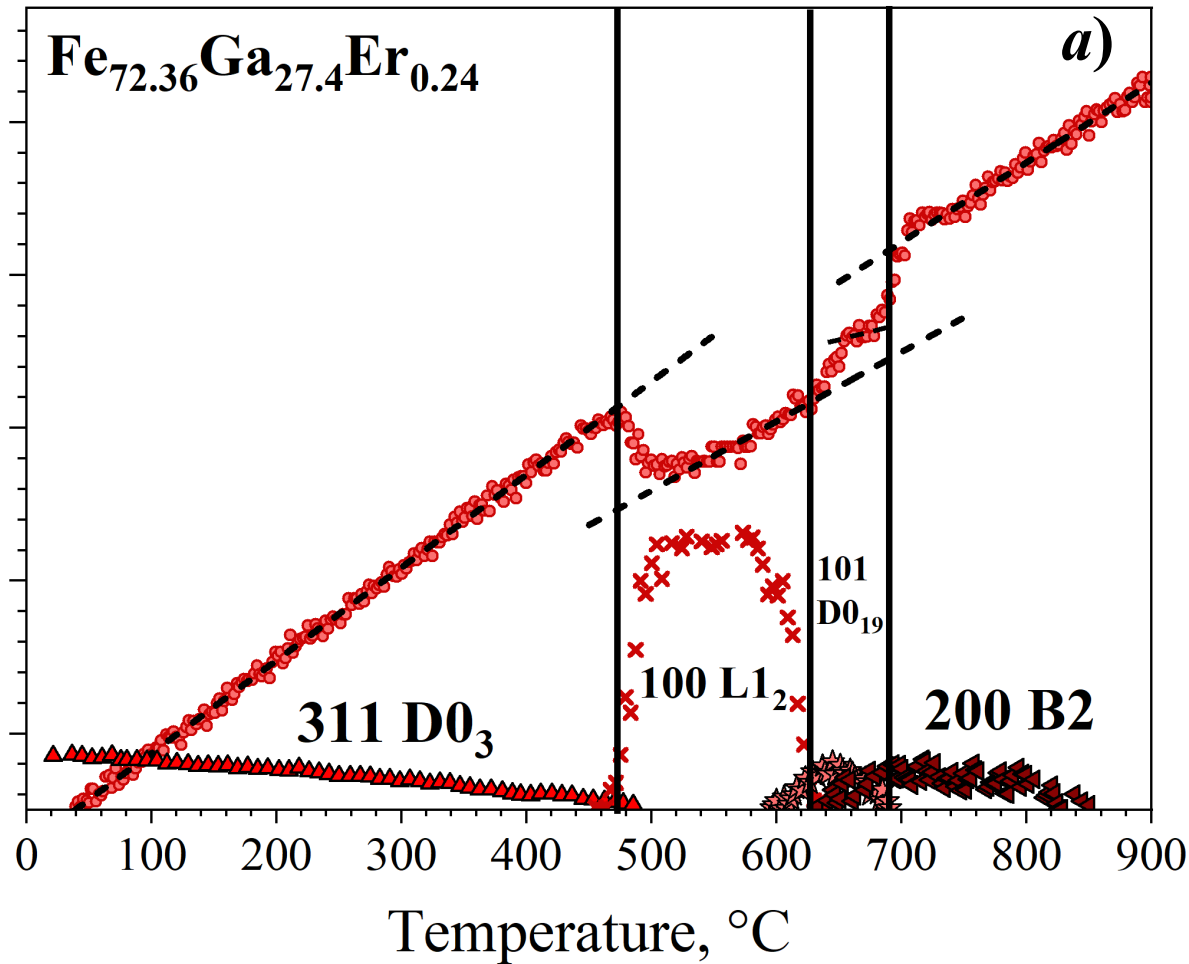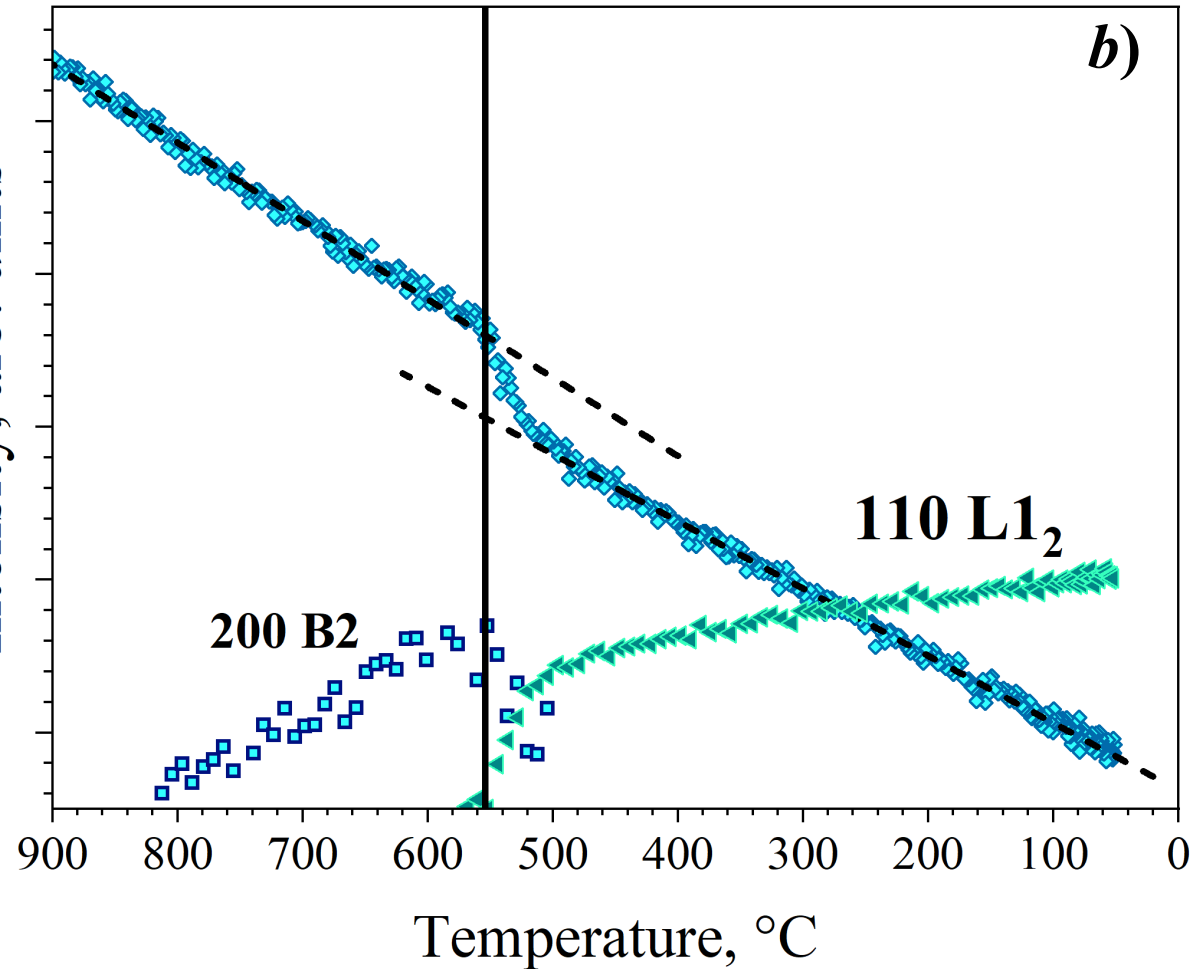On plots we can observe the deviation of the lattice parameter values from a linear dependence upon disordering, which clearly correlates with the behavior of the intensity of the superstructural peaks 311, 200 of the $D0_3$, B2 phases. Deviations of the atomic volume begin somewhat earlier and end later than the disappearance of the superstructural peak

Analysis of the data of the thermodiffractometric experiment
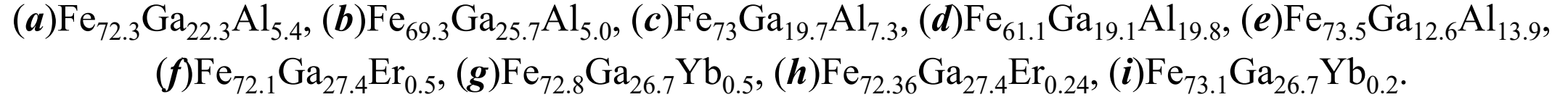

Temperature dependence of the diffuse background averaged over the interval d = (2.6 – 2.8) Å, measured during heating **a)** and cooling **b)**. The change in the slope of the dependence correlates with phase transitions during heating and cooling, which is determined by the intensity of the peaks of these phases.

Conclusion

The following alloy compositions have been investigated :

$(a)\text{Fe}_{72.3}\text{Ga}_{22.3}\text{Al}_{5.4}$, $(b)\text{Fe}_{69.3}\text{Ga}_{25.7}\text{Al}_{5.0}$, $(c)\text{Fe}_{73}\text{Ga}_{19.7}\text{Al}_{7.3}$, $(d)\text{Fe}_{61.1}\text{Ga}_{19.1}\text{Al}_{19.8}$, $(e)\text{Fe}_{73.5}\text{Ga}_{12.6}\text{Al}_{13.9}$, $(f)\text{Fe}_{72.1}\text{Ga}_{27.4}\text{Er}_{0.5}$, $(g)\text{Fe}_{72.8}\text{Ga}_{26.7}\text{Yb}_{0.5}$, $(h)\text{Fe}_{72.36}\text{Ga}_{27.4}\text{Er}_{0.24}$, $(i)\text{Fe}_{73.1}\text{Ga}_{26.7}\text{Yb}_{0.2}$.

1. It was found that in the initial (as cast) state, alloys with a total content of Ga, Al metals is less than 31 at. % (alloys a, b, c, e with $x + y \leq 31$) are characterized by a mixture of partially ordered phases B2 and D0$_3$, alloys f, g, h are characterized by one phase D0$_3$, alloy i is in a mixture of phases D0$_3$ + L1$_2$, and alloy d ($x + y = 38.9$) in phase B2. The two-phase state observed in alloys a, b, c, e is organized as a matrix, which is played by the B2 phase, in which clusters of the D0$_3$ phase are dispersed.

2. The Pielaszek method, which allow to determine the values and distributions of grain size along the diffraction line profile, is implemented as a computer program.

3. The broadening of the range of formation of cubic phases based on the bcc cell in ternary alloys as compared to $\text{Fe}_{100-x}\text{Ga}_x$ indicates the role of Al in the stabilization of these structures. And doping of Fe-Ga alloys with rare-earth elements in an amount of 0.5% at. led to partial or complete stabilization of cubic structures based on a bcc cell.

4. The m-D0$_3$ phase, which has been reliably observed using electron microscopy and diffraction techniques, was not observed in the neutron diffraction spectra obtained from the investigated FeGa-based alloys.

Phase separation at different length scales in *Galfenol* related alloys

FLNP group
A.M. Balagurov, head of the project
T.N. Vershinina
N.Yu. Samoylova
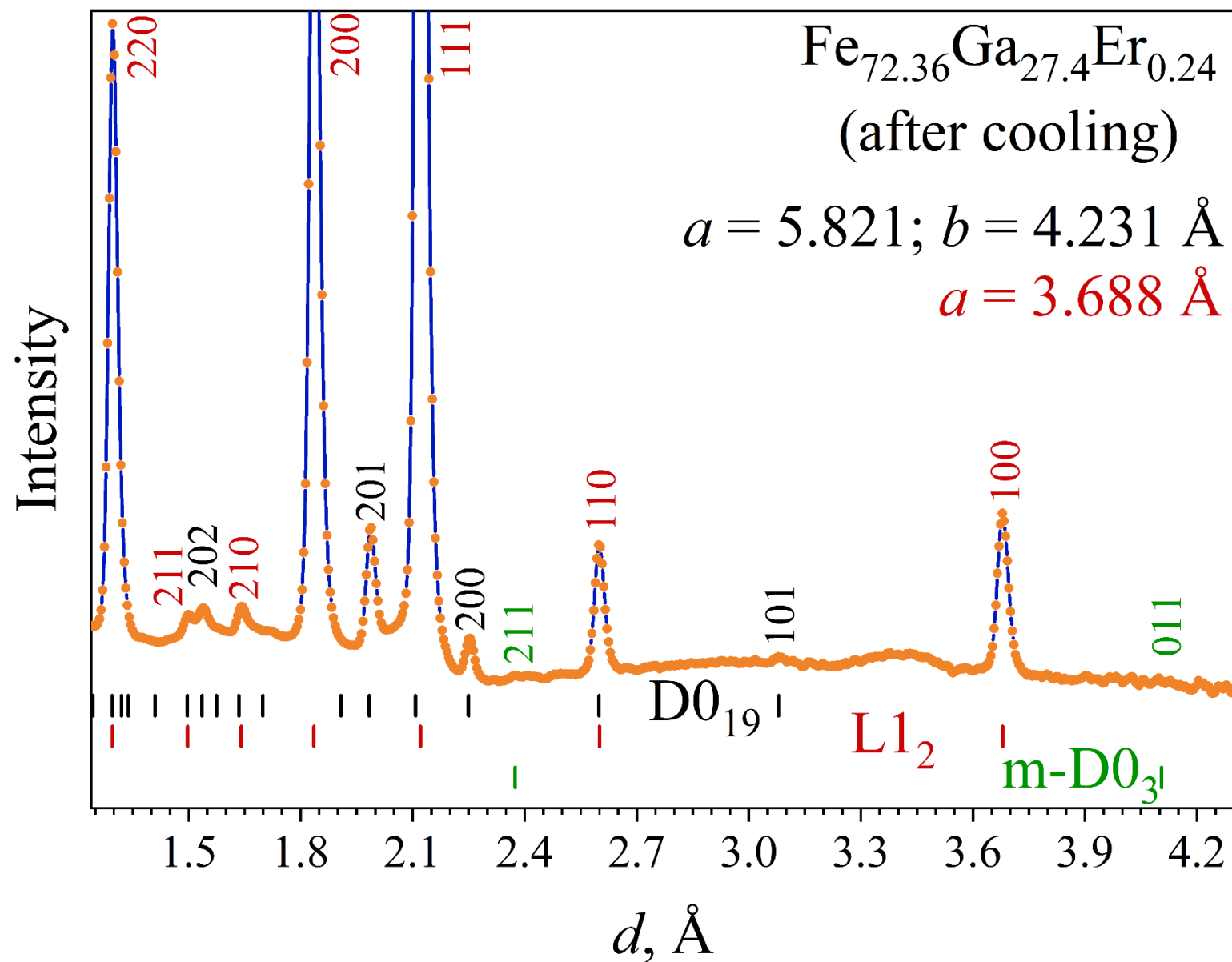A.S. Sohackij
S.V. Sumnikov
B. Muhametuly
B. Yerzhanov

MISIS group
I.S. Golovin, head of the group
V.V. Palacheva
A.A. Scherbakov

Medium resolution neutron diffraction spectrum

Fe$_{72.36}$Ga$_{27.4}$Er$_{0.24}$
(after cooling)

$a = 5.821$; $b = 4.231$ Å

$a = 3.688$ Å

Intensity

d, Å

220 200 111 211 202 210 201 200 211 110 101 100 011

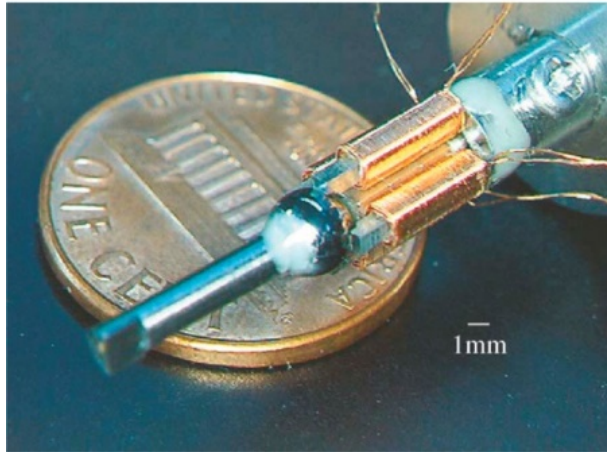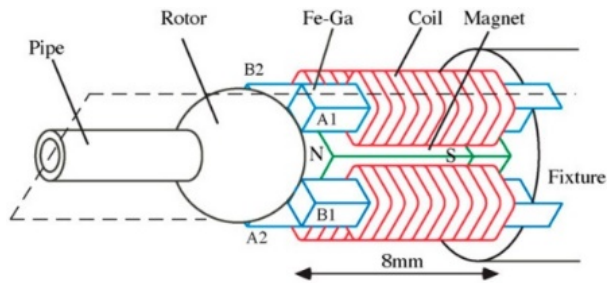D0$_{19}$ L1$_2$ m-D0$_3$

1

Results of thermodiffractometry

A number of first and second order phase transition in Fe-Ga based alloys during slow heating and cooling are presented.

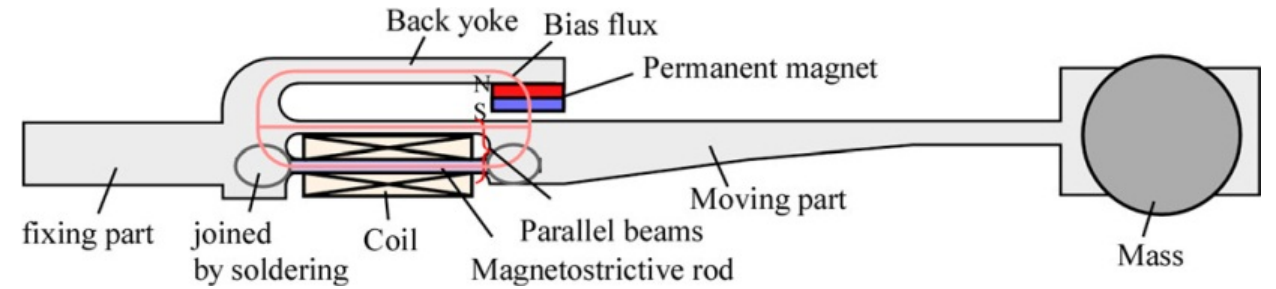| Sample composition, at.%	Heating	Cooling
$Fe_{73.5}Ga_{12.6}Al_{13.9}$	B2+D0$_3$ → B2 → A2	A2 → B2 → B2+D0$_3$
$Fe_{72.3}Ga_{22.3}Al_{5.4}$	B2+D0$_3$ → B2 → A2	A2 → B2 → B2+D0$_3$
$Fe_{73}Ga_{19.7}Al_{7.3}$	B2+D0$_3$ → B2 → A2	A2 → B2 → B2+D0$_3$
$Fe_{69.3}Ga_{25.7}Al_{5.0}$	B2+D0$_3$ → D0$_3$+A1 → B2+A1 → B2 → A2	A2 → B2 → B2+D0$_3$
$Fe_{72.1}Ga_{27.4}Er_{0.5}$	D0$_3$ → D0$_3$+A1 → D0$_3$+A3 → A2	A2 → D0$_3$
$Fe_{72.8}Ga_{26.7}Yb_{0.5}$	D0$_3$ → A2	A2 → D0$_3$
$Fe_{72.36}Ga_{27.4}Er_{0.24}$	D0$_3$ → L1$_2$→ D0$_{19}$ → B2 →A2	A2 → B2 → D0$_3$→ L1$_2$+ D0$_{19}$
$Fe_{73.1}Ga_{26.7}Yb_{0.2}$	D0$_3$+L1$_2$ → L1$_2$ → D0$_{19}$+A1 → L1$_2$	A2+L1$_2$→ B2+L1$_2$ → L1$_2$+ D0$_{19}$+A2

Once upon a time, the microstructure of a crystalline substance meant what is visible under a microscope, for example, grains in alloys. With the advent of diffraction, **microstructure** began to be understood as the following characteristics: **crystallographic texture, the level of residual stresses in crystallites (macro- and microstresses), the amount of mosaic (for single crystals) and the coherently scattering domain size**. For ordering alloys, an important feature of the microstructure is also the morphology of the ordered regions, their size distribution and the level of order in them, as well as the characteristics of local ordering.
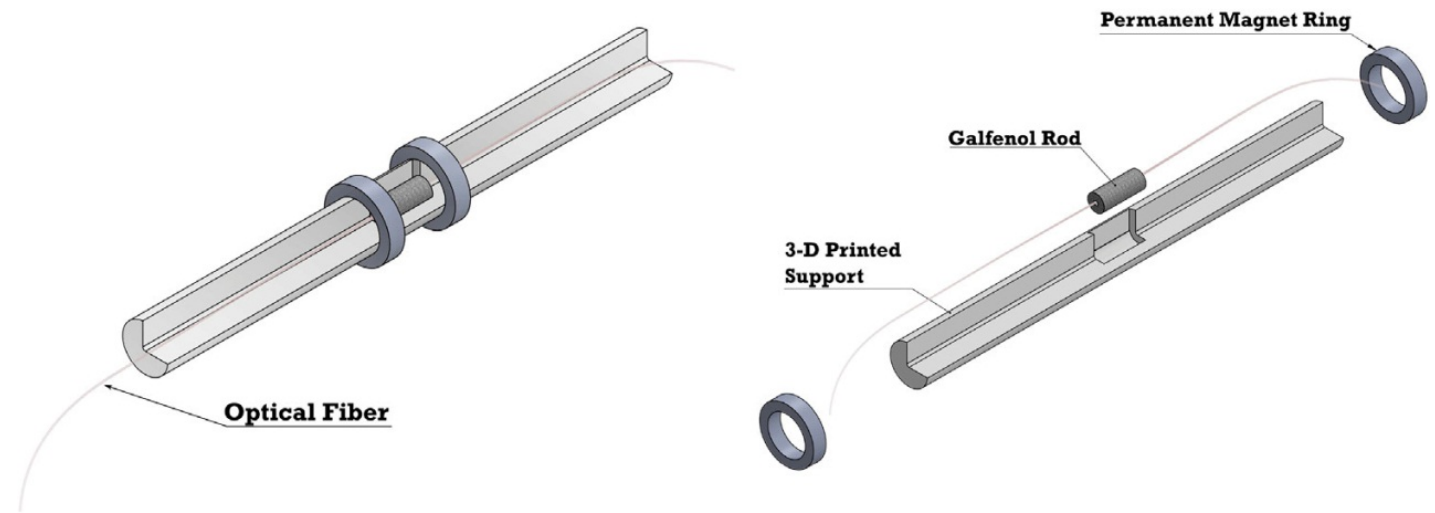
Application of galfenols

Galfenol electricity generator based on vibration absorption.

Miniature spherical motor based on galfenol.

Galfenol magnetic field sensor.

2. Miniature spherical motor using iron–gallium alloy (Galfenol) / T. Ueno, T. Higuchi, C. Saito, N. Imaizumi

3. Performance of improved magnetostrictive vibrational power generator, simple and high power output for practical applications / T. Ueno

4. A magnetostrictive biased magnetic field sensor with geometrically controlled full-scale range / V. Apicella, C. Visone [et al.]

All phase transitions were recorded by the appearance and disappearance of reflections related to a certain phase. For three possible structural states $D0_3$, B2 and A2, diffraction reflections can be divided into three groups (unit cell $D0_3$ is used for indexing):

- intense (fundamental) reflections with even Miller indices (h, k, l) and $(h+k+l) = 4 = 4n$, allowed in all three phases;

- weaker reflections with even (h, k, l) and odd $(h+k+l) = 2 = 2n$, allowed in phases $D0_3$ and B2;

- weak (superstructural) reflections with odd (h,k,l), which are allowed only in the $D0_3$ phase.

Magnetostriction is assessed by a dimensionless quantity - a relative change in the size of the sample $\lambda = \frac{\Delta l}{l}$, where **Δl** is the elongation (or shortening) when a magnetic field is turned on, and l is the length of the sample. Usually in experiments two units are measured: $\lambda_{\parallel}$ and $\lambda_{\perp}$, where $\lambda_{\parallel}$ – transverse magnetostriction, and $\lambda_{\perp}$ – longitudinal magnetostriction. Transverse magnetostriction is measured when the field strength coincides with the direction of magnetostriction measurement, and longitudinal magnetostriction when the directions are mutually perpendicular. These magnetostriction units are related to each other as: $\lambda_{\perp} = -\lambda_{\parallel}/2$. There are isotropic and anisotropic magnetostriction. In cubic crystals, anisotropic magnetostriction is usually characterized by two main constants λ_{100} and λ_{111}, that is, the relative change in crystal size in the [100] and [111] directions upon magnetization occurs in the same directions. The constants λ_{100}, λ_{111} can be either positive or negative. In the literature, it is customary to give the values $\lambda_1 = (3/2)\lambda_{100}$ and $\lambda_2 = (3/2)\lambda_{111}$, which are included as coefficients in the expansion of magnetostriction in terms of the components of the magnetization vectors and measurement direction. For a polycrystalline material, averaging is carried out over various crystallographic directions and the value λ_S is given, the magnetostriction constant when the magnetization reaches saturation.
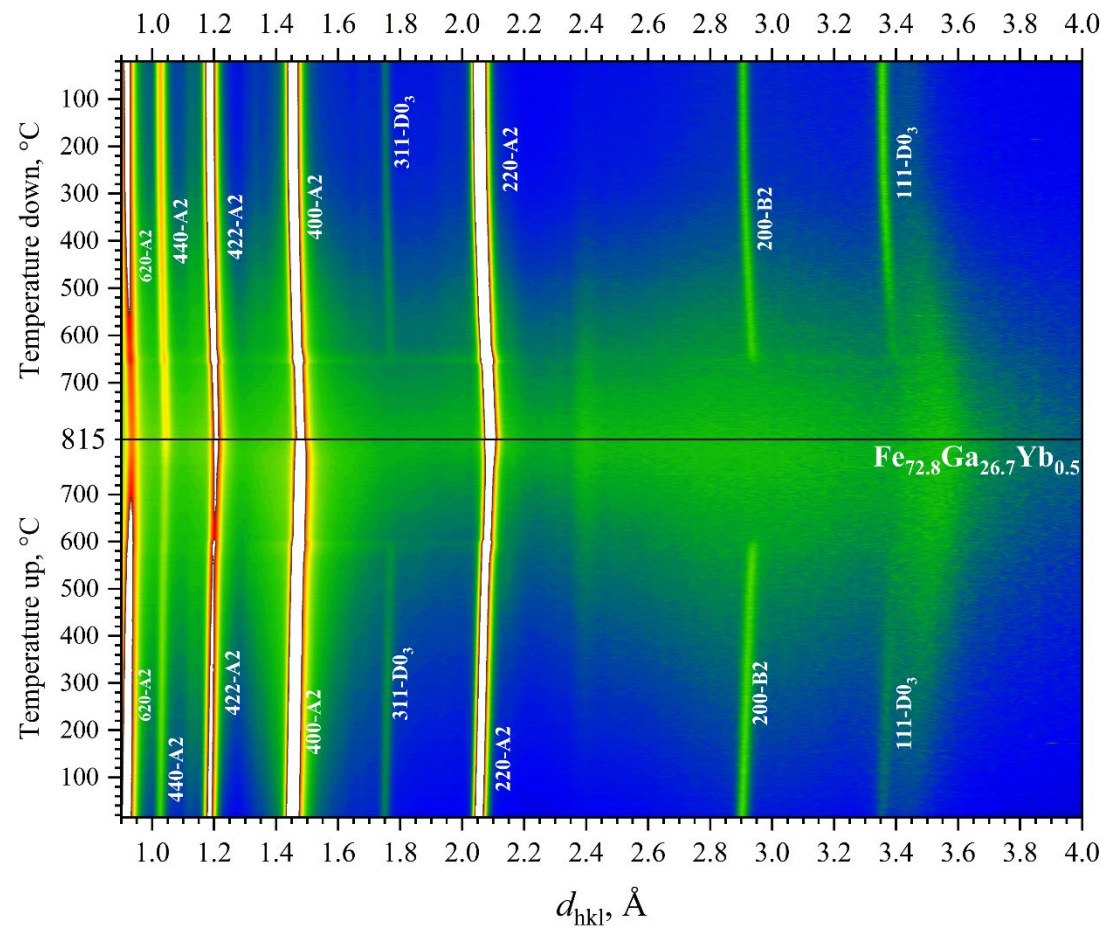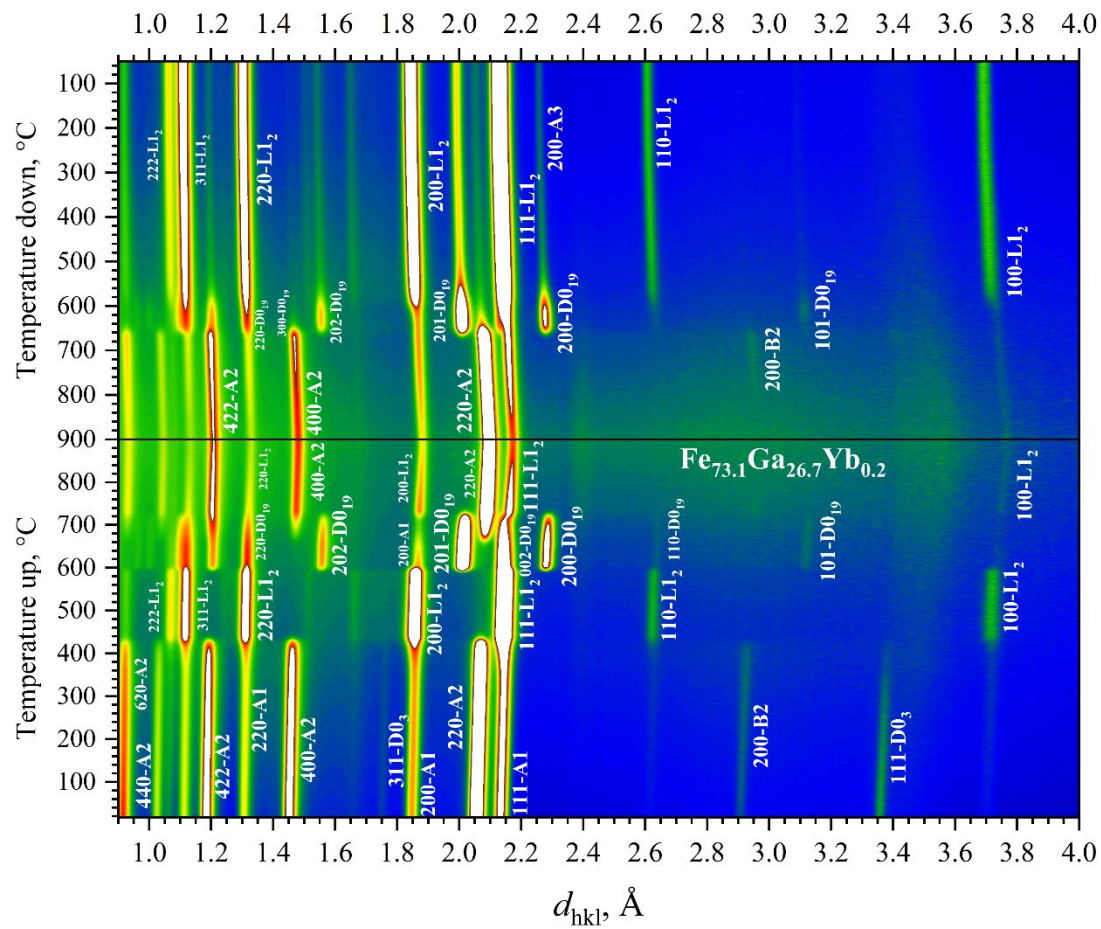
The basis for assumptions about the cause of giant magnetostriction in Fe-Ga alloys is the volumetric phase inhomogeneity of the material, consisting of nanoprecipitates of one of the ordered clusters in a disordered or less ordered matrix

It is assumed that the main reasons determining the increase in magnetostriction of alloys with additions of RE elements are:

- the presence of strong magnetic anisotropy in some elements (especially Tb) the formation of local
- microstresses in crystallites around RE ions and the formation of nanoinhomogeneities, often interpreted as tetragonal phases m-D0$_3$ (modified-D0$_3$) and D0$_{22}$

Fe₇₃.₁Ga₂₆.₇Yb₀.₂   Fe₇₂.₈Ga₂₆.₇Yb₀.₅

Scherrer, Stokes-Wilson and Williamson-Hall methods

$$\Delta d_D = d^2/D_{coh}$$ **(1)**

$$\Delta d_\varepsilon = 2\varepsilon \cdot d$$ **(2)**

$$\Delta H_D = 1/D_{coh}$$ **(3)**
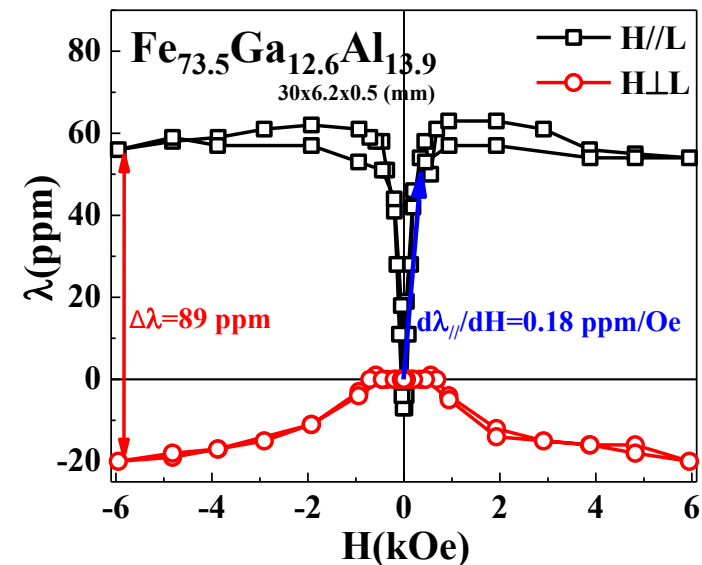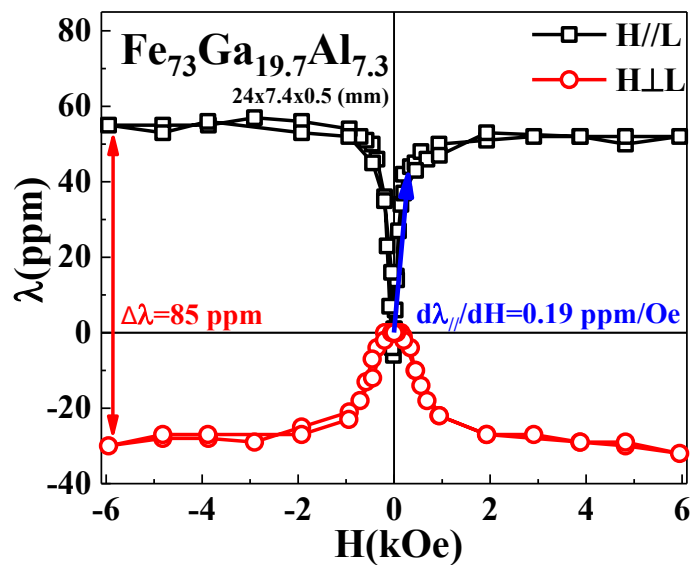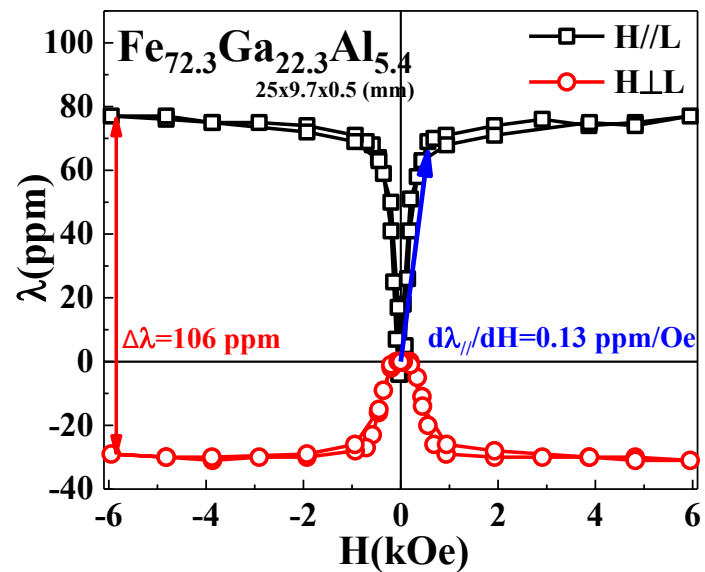
$$\Delta H_\varepsilon = 2\varepsilon \cdot H$$ **(4)**

- D_{coh} is the effective size of coherent scattering regions averaged over the sample volume in the direction parallel to the scattering vector;

- ε is the magnitude of microstresses;

- d—interplanar distance;

- Δd—peak width at half maximum (in the scale of interplanar distances);

- $H = 1/d$ is the length of the vector in reciprocal space;

- ΔH is the peak width at half maximum (in reciprocal space vector scale).

Microstructure: dimensional and deformation effects

$$(\Delta d)^2 = C_1 + C_2 d^2 + C_3 d^2 + C_4 d^4$$ **(5)**

$$(\Delta H)^2 = C_4 + C_3 H^2 + C_2 H^2 + C_1 \cdot H^4$$ **(6)**

TOF diffractometer resolution function $\longrightarrow$ $(Al_2O_3, La^{11}B_6)$ Standard sample

Microdeformations, $C_3 = 2\varepsilon = 2\Delta a/a$

Dimensional effects, $C_4 \sim (1/L)^2$

	$Fe_{72.3}Ga_{22.3}Al_{5.4}$	$Fe_{73}Ga_{19.7}Al_{7.3}$	$Fe_{73.5}Ga_{12.6}Al_{13.9}$
Taiwan λ (ppm)	≈ 79	≈ 55	≈ 55
Russia λ (ppm)	70	58	53.2

11

Распределение по размерам (гамма и логнормальное распределение).

Гамма распределение:

$G(x) = R_0^{-(m + 1)} \cdot x^m \cdot \exp(-x/R_0)/\Gamma(m + 1),$

где $\Gamma(z) = \int_0^\infty t^{z-1}\exp(-t)dt$ – гамма-функция Эйлера, $x > 0$.

Среднее значение размера ОКР, $<R>$, и дисперсия, σ^2, распределения $G(x)$ связаны с его параметрами так:

$<R> = (m + 1)R_0$, $\sigma^2 = (m+1)R_0^2$; $R_0 = \sigma^2/<R>$, $m = <R>^2/\sigma^2 - 1$.

Усредненный по объему размер ОКР вычисляется по формуле:

$<R>_{VG} = (<R>^2/\sigma^2 + 3) \cdot (\sigma^2/<R>) = <R> + 3\sigma^2/<R>$.